Hydroxychloroquine enhances the antitumor effects of BC001 in gastric cancer

WEI WANG[1*], LINQING LIU[2*], YUCHENG ZHOU[3], QIANG YE[1], XIULI YANG[1],
JINYING JIANG[1], ZIQI YE[4], FENG GAO[5], XIAOLU TAN[5],
GUOBING ZHANG[1], QINGXIA FANG[1] and ZIXUE XUAN[1]

[1]Department of Pharmacy, Zhejiang Provincial People's Hospital, People's Hospital of Hangzhou Medical College,
Hangzhou, Zhejiang 310014; [2]Department of Geriatrics, The First Affiliated Hospital of USTC,
Division of Life Sciences and Medicine, University of Science and Technology of China, Hefei,
Anhui 230001; [3]Department of General Surgery, Key Laboratory of Gastroenterology of Zhejiang,
Zhejiang Provincial People's Hospital, Hangzhou, Zhejiang 310014; [4]Department of Pharmacy,
The First Affiliated Hospital, College of Medicine, Zhejiang University, Hangzhou, Zhejiang 310003;
[5]Buchang (Beijing) Pharmaceutical R&D Co., Ltd., Beijing 100176, P.R. China

Abstract. Gastric cancer is an important cancer type worldwide, the anti-angiogenic agent BC001 can target the vascular endothelial growth factor receptor 2 (VEGFR2), and significantly suppresses the growth of gastric cancer BGC823 cells *in vitro* and *in vivo*. However, numerous results indicated that antiangiogenic drugs could induce autophagy, and the inhibition of autophagy enhanced the anticancer effects of antiangiogenic agents. In the present study, hydroxychloroquine (HCQ), an inhibitor of autophagy, enhanced the antiproliferative and proapoptotic effects of BC001 *in vitro*. Furthermore, HCQ enhanced the antitumor effects of BC001 on BGC823 xenograft tumors *in vivo*. Of note, BC001 neither induced nor inhibited autophagy. RNA-sequencing results revealed that HCQ regulated autophagy or lysosomal-associated genes, such as tumor protein p53-inducible nuclear protein 1, interleukin (IL)1B, tumor necrosis factor (TNF), Mediterranean fever, ubiquitin specific peptidase 36, IL6, neuraminidase (NEU)1, ATP-binding cassette subfamily A member 1, proprotein convertase subtilisin/kexin type 9, myelin basic protein and NEU3. Importantly, HCQ was determined to affect multiple pathways, including 'negative regulation of endothelial cell proliferation', 'blood vessel remodeling', 'cell surface receptor signaling pathways' and 'notch receptor processing' associated with 'signal transduction', 'cancers' and 'immune system', through regulating C-X-C motif chemokine ligand 8, TNF, IL6, intercellular adhesion molecule 1 and FOS genes. In summary, HCQ was proposed to enhance the anticancer effects of BC001 in gastric cancer via complex mechanisms.

Introduction

According to global cancer statistics 2018, gastric cancer remains an important cancer type worldwide, as it is the fifth most frequently diagnosed cancer and the third leading cause of cancer-associated mortality in the world (1). Previously, the only treatment choice for patients with advanced gastric cancer was chemotherapy (2); however, the efficacy of chemotherapy is limited, and increased evidence suggests that the growth, invasion and metastasis of tumor rely on tumor angiogenesis, which regulated by the vascular endothelial growth factors (VEGFs) and corresponding receptors (3). Bevacizumab is an anti-VEGF monoclonal recombinant humanized antibody, which is approved by the Food and Drug Administration (FDA) to treat colorectal, breast, lung, renal, ovarian cancers and glioblastoma (4). As a monoclonal antibody that recognizes and binds to VEGF receptor 2 (VEGFR2), ramucirumab is the only anti-angiogenic agent approved by the FDA for the treatment of patients with advanced gastric cancer (5).

BC001 is a novel fully humanized monoclonal antibody of VEGFR2. Our previous study showed that BC001 inhibited the growth of gastric cancer *in vitro* and *in vivo* (6); however, an AVAGAST trial showed that bevacizumab combined with chemotherapy could not significantly improve overall survival of patients with advanced gastric cancer, indicating that it is important to identify an effective BC001-combined therapeutic regimen for the treatment of gastric cancer (7). Numerous

Correspondence to: Professor Zixue Xuan, Department of Pharmacy, Zhejiang Provincial People's Hospital, People's Hospital of Hangzhou Medical College, Hangzhou, Zhejiang 310014, P.R. China
E-mail: xuanzixue0222@163.com

*Contributed equally

studies have demonstrated that certain anti-angiogenic drugs could induce autophagy (8-10).

Hydroxychloroquine (HCQ), an anti-malarial drug, efficiently inhibits cellular lysosomal functions, and enhances the anticancer effects of other therapeutic agents (11,12). Evidence has suggested that therapies combined with HCQ are better at producing positive anticancer effects than HCQ or therapy alone (13). Although, whether HCQ promotes the anticancer effect of BC001 in gastric cancer and whether BC001 induces autophagy remain unclear.

In the present study, we reported that HCQ enhanced the antiproliferative and proapoptotic properties of BC001 *in vitro*, and promoted the antitumor effects of BC001 on a BGC823 cell-based xenograft tumor *in vivo*. Our data also revealed that BC001 did not influence autophagy, whereas HCQ could inhibit autophagy by impairing autophagosome fusion with lysosomes and induced severe ultrastructural changes, which may contribute to the impaired fusion. To increase our understanding of the mechanisms, RNA-sequencing (RNA-Seq) was used to analyze alterations in gene expression following combined treatments and single drug treatment. The results showed that the expression of numerous autophagy-associated genes were altered in HCQ-treated cells, including tumor protein p53-inducible nuclear protein 1 (TP53INP1), interleukin (IL)1B, tumor necrosis factor (TNF), Mediterranean fever (MEFV), ubiquitin specific peptidase 36 (USP36), IL6, and lysosome-associated genes also were changed, such as neuraminidase (NEU)1, ATP-binding cassette subfamily A member 1 (ABCA1), proprotein convertase subtilisin/kexin type 9 (PCSK9), myelin basic protein (MBP) and NEU3. In addition, HCQ also affects multiple pathways, including negative regulation of endothelial cell proliferation, blood vessel remodeling, cell surface receptor signaling pathways and notch receptor processing in signal transduction, cancers and immune system. C-X-C motif chemokine ligand 8 (CXCL8), TNF, IL6, ICAM1 and FOS may be 'hub' genes. Therefore, our findings suggested that HCQ may enhance the anticancer effects of BC001 in gastric cancer via complex mechanisms.

Materials and methods

Cell culture. The human gastric cancer cell line BGC823 was obtained from the American Type Culture and Collection, and was cultured in Dulbecco's modified Eagle's medium (Gibco; Thermo Fisher Scientific, Inc.), supplemented with 10% fetal bovine serum (FBS, Gibco; Thermo Fisher Scientific, Inc.). BGC823 cells were cultured at 37°C in a humidified atmosphere containing 5% CO_2.

Reagents and antibodies. The antibodies for microtubule-associated light chain 3 (LC3) (cat. no. 12741s) and cleaved-caspase-3 (cat. no. 9664s) were purchased from Cell Signaling Technology, Inc. p62 (cat. no. Ab109012), Ki67 (cat. no. Ab16667), and caspase-3 (cat. no. Ab32351) antibodies were obtained from Abcam. Anti-CD31 (cat. no. AF6191) was obtained from Affinity. Hydroxychloroquine (HCQ) was purchased from Sigma-Aldrich (Merck KGaA); Annexin V-fluorescein isothiocyanate (FITC) Assay kit was from BD Biosciences, Cell Counting Kit-8 (CCK-8, cat. no. CK04) was purchased from Dojindo Molecular Technologies, Inc.,

and TRIzol® (cat. no. 9109) was purchased from Thermo Fisher Scientific, Inc.

CCK-8 cell viability assay. A CCK-8 kit was used to detect the effects of HCQ on the proliferation of BGC823 cells. Briefly, cells (2.0×10^4 cells/ml) were seeded onto 96-well plate. After incubation at 37°C for 24 h, cells were treated with different concentrations of HCQ (0, 2, 4, 6, 8, 16, 32, 64, 128, and 256 µg/ml) for 24 h. Then, 10 µl CCK-8 reagent was added to each well and incubated at 37°C for another 1 h. The optical density (OD) was measured at 450 nm using a microplate reader. Cell proliferation inhibition rate = (1-OD of the treatment group/OD of the control group) x 100%.

Real-time cell analyzer (RTCA) assays. Briefly, 50 µl of cell culture medium supplemented with FBS was added into each well of the E-plate 96 that was then connected to the system to obtain background impedance readings. Cell suspensions (50 µl, 3×10^4 cells/ml) were seeded in E-plate 96 followed by incubation at 37°C with 5% CO_2. When the cells reached the logarithmic growth phase, BC001 (20 µg/ml) or HCQ (5 µg/ml) alone or in combination, were added to the wells of E-plate 96. The control group (CK) received no treatment. The plate was then incubated at room temperature for 30 min and then placed on the RTCA SP Station for continuous impedance recording every 2 min (14).

Flow cytometry. The cells were seeded in 6-well plates and were treated with BC001 (20 µg/ml) or HCQ (5 µg/ml) alone or in combination for 24 h. Untreated cells were used as a negative control. After washing with PBS twice and subsequent by trypsinization, the cells were resuspended in 500 µl of binding buffer (BD Biosciences) supplemented with 5 µl of Annexin V-FITC and 5 µl of propidium iodide (PI) according to the manufacturer's recommendations. Finally, the fluorescence intensity of the samples was determined by flow cytometry (EPICS XL-MCL, Beckman Coulter, Inc.), and the number of apoptotic cells in each sample was analyzed using FCS Express version 3.0 (De Novo Software). The whole experiment was performed in triplicate.

Western blotting. Proteins of cells treated with BC001 (20 µg/ml) or HCQ (5 µg/ml) alone or in combination for 24 h, were extracted using radioimmunoprecipitation assay lysis buffer (Roche Diagnostics), and protein concentrations were measured using a BCA assay. The samples (20 µg/lane) were subjected to 10% SDS-PAGE gels, and then transferred to a PVDF membrane. After blocking with 5% non-fat milk ~1 h at room temperature, the membrane was incubated with indicated antibodies (LC3B, 1:2,000; p62, 1:1,000; GAPDH, 1:10,000) for 2 h at room temperature. Then, the membrane was washed three times with TBST buffer, and incubated with the horseradish peroxidase-conjugated goat anti-rabbit secondary antibodies (cat. no. 7074, Cell Signaling Technology, Inc., 1:10,000) at room temperature for 1 h. The reaction was visualized using ECL (cat. no. 170-5060, Bio-Rad Laboratories, Inc.) and detected by exposure to autoradiographic film. Immunoreactive products were visualized using ECL and quantified by densitometry using ImageJ software (version 1.50, National Institutes of Health).

mCherry-enhanced green fluorescent protein (EGFP)-LC3 immunofluorescence. To further analyze how HC001 or HCQ affected the stepwise progression of autophagy, BGC823 cells were transfected with 2.5 μg the plasmid expressing mCherry-EGFP-LC3 using Lipofectamine® 3000 (Invitrogen; Thermo Fisher Scientific, Inc.) in 6-well plate according to the manufacturer's instructions. Then, BGC823 cells expressing mCherry-EGFP-LC3 were added to plates. After 24 h, these cells were treated with BC001 (20 μg/ml) in the absence or presence of HCQ (5 μg/ml) at 37°Cfor 24 h. After treatment, cells on the coverslips were fixed with 1% PFA in PBS for 15 min in the dark at room temperature, and washed with PBS thoroughly. The autophagic flux was measured using a laser scanning confocal microscope (LSM880, Zeiss AG) (15,16).

Transmission electron microscopy. After treatment with 20 μg/ml BC001 and/or 5 μg/ml HCQ, BGC823 cells were washed with PBS twice and fixed in glutaraldehyde (3.5% in 0.1 mol/l cacodylate buffer, pH 7.4) at 4°C for 24 h, respectively. Then, BGC823 cells were post-fixed with 1% osmium tetroxide (OsO_4) at 4°C for 30 min and embedded in epoxy resins. Uranyl acetate (saturated uranyl acetate in 50% alcohol) and lead citrate (1% lead citrate in H_2O) were applied for staining ultrathin sections, and examined with transmission electron microscopy (H-7650, Hitachi Ltd.) (17).

RNA-Seq and bioinformatics analysis. Total RNA (1 μg for each sample) was extracted from BC001 or/and HCQ-treated BGC823 cells using TRIzol according to the manufacturer's instructions. cDNA libraries were prepared, and the library products were then ready for sequencing analysis via an BGISEQ-500 platform (Beijing Genomics Institute). After raw reads were subjected to quality control testing using Soapnuke software (version 1.4.0, clean reads were matched to the reference genome. Following alignment, the RSEM tool (version 2.2.5, https://deweylab.github.io/RSEM/) was used for transcript quantification, and the fragments per kilobase million (FPKM) method was performed to calculate the expression level. Genes with FPKM<10 were identified for differential expression analysis. Based on the detection results, differentially expressed genes (DEGs) were also analyzed by hierarchical clustering using pheatmap function in R software(version 3.5.1, https://www.r-project.org/); the hypergeometric test and false discovery rate (FDR) correction methods were also employed. Finally, we used Gene Ontology (GO; http://geneontology.org/) and Kyoto Encyclopedia of Genes and Genomes (KEGG; https://www.genome.jp/kegg/) pathway enrichment analyses to study the mechanism underlying the HCQ-enhanced anticancer effects of BC001 in gastric cancer (18,19). In our analysis, we identified DEGs between samples using the following criteria: FDR≤0.001 and a log2-fold change ratio ≥1.

Animal experiments. BGC823 cells ($1.5x10^6$ cells/ml) were subcutaneously injected into the right flanks of the mice (nu/nu, female, 6-8 weeks, 18-22 g, Vital River Laboratories Co., Ltd.). Mice were housed in the laboratory under specific pathogen-free conditions: Temperature, 22-25°C; humidity, 50-60%; 12-h light/dark cycle. Mice had free access to water and Purina 5L79 rodent chow (Nestlé Purina PetCare Company). Once the tumors reached a measurable size, these mice were randomly assigned to one of the following four groups: i) Control, mice received an intraperitoneal injection of PBS five times a week; ii) BC001, mice received an intraperitoneal injection of BC001 5 mg/kg two times a week; iii) HCQ, mice received an intraperitoneal injection of HCQ 5 mg/kg five times a week; and iv) combination, mice were treated with intraperitoneal injection of BC001 (5 mg/kg two times a week) and HCQ (HCQ 5 mg/kg five times a week). After 4 weeks of treatment, tumor size was measured via two perpendicular dimensions with calipers, then tumor volume was calculated using the formula: $(ab^2)/2$; 'a' represents the length and 'b' represents the width of tumor, respectively. Finally, mice were euthanized with an intraperitoneal injection of pentobarbital sodium (200 mg/kg) at the end of the experiment, then tumors were harvested and weighed. The expression of Ki67, caspase-3, cleaved-caspase-3, and CD31 in xenograft tumors was also detected by immunohistochemistry (IHC) staining (6).

Statistical analysis. The results were presented as the mean ± standard deviation of at least 3 independent experiments, and statistical comparisons between groups were determined by one-way analysis of variance or Student's t-test followed by a Tukey's post hoc test to determine the significant differences of means in two or multiple groups (n>2) comparisons. P<0.05 was considered to indicate a statistically significant difference.

Results

HCQ promotes the antitumor effects of BC001 in vitro. The effects of combined therapy of HCQ and BC001 against gastric cancer remains unknown. Here, we investigated the effects of HCQ alone or together with BC001 on gastric cancer cell line, BGC823. As shown in Fig. 1A, HCQ alone could inhibit BGC823 cells in a dose-dependent manner, with a half-inhibitory concentration of 52.95±6.82 μg/ml. In addition, the results from RTCA data showed that BC001 (20 μg/ml) or HCQ (5 μg/ml) alone could decrease the cell index; the cell index of cells treated by HCQ and BC001 combined was the lowest, indicating that BC001 and HCQ could inhibit BCG823 proliferation. Of note, HCQ significantly enhanced the anti-proliferative effect of BC001 (Fig. 1B). In addition, we investigated whether HCQ could promote BGC823 apoptosis together with BC001. Cell apoptosis was analyzed by fluorescence-activated cell sorting using Annexin V-FITC/PI staining after treatment with HCQ, BC001 alone or in combination. The results revealed that BC001 did not appear to significantly promote apoptosis compared with the control, while HCQ could enhance apoptosis induced by BC001 (Fig. 1C and D).

HCQ enhances the anticancer activity of BC001 in vivo. To investigate the *in vivo* efficacy of the combined treatment of HCQ and BC001 in gastric cancer, a BGC823 xenograft tumor model was established in nude mice. As presented in Fig. 2, significant tumor growth suppression was observed in the HCQ and BC001 treatment groups compared with the control. In addition, the tumor volume and size of the combination group were significantly reduced, compared with the control (Fig. 2A and B). We also analyzed the expression of Ki67, caspase-3, cleaved-caspase-3 and CD31 in tumor tissues using
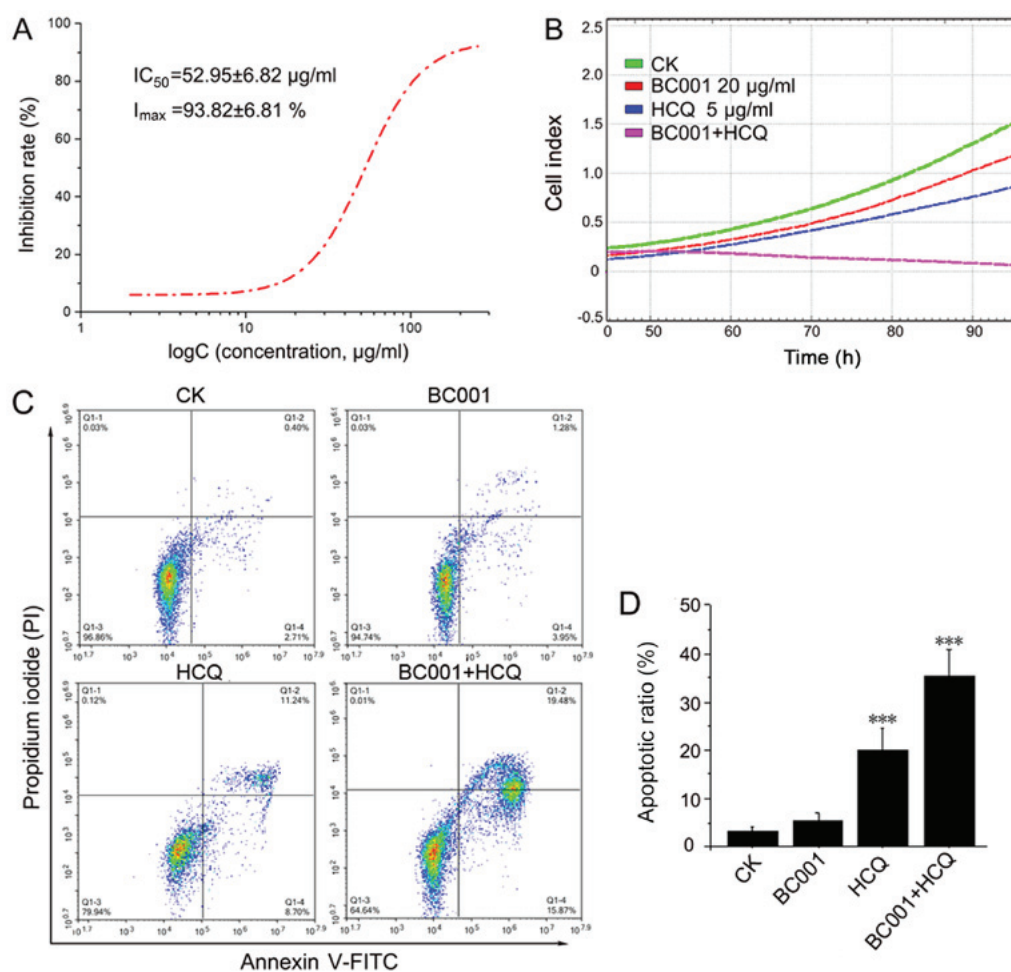
Figure 1. HCQ promotes the antitumor effects of BC001 *in vitro*. (A) HCQ inhibited BGC823 cell viability in a dose-dependent manner using a Cell Counting Kit-8 assay; (B) HCQ enhanced the anti-proliferative effects of BC001 on BGC823 cells as determined with a Real-time cell analyzer System. (C) HCQ promoted the apoptosis of BGC823 cells following BC001 treatment as determined by flow cytometry. (D) Apoptosis ratio of cells treated with HCQ and/or BC001. ***$P<0.001$ vs. CK. CK, control group; FITC, fluorescein isothiocyanate; HCQ, hydroxychloroquine; I_{max}, maximal inhibitory concentration; IC_{50} half-maximal inhibitory concentration.

IHC. Compared with the untreated and single drug-treated groups, cleaved-caspase-3 expression was increased, while Ki67 and CD31 expression was reduced in the combination group (Fig. 2C). This indicated that HCQ also increased the anticancer effects of BC001 *in vivo* by inhibiting cell growth and promoting apoptosis.

Autophagy is not influenced by BC001, but is affected by HCQ, which leads to ultrastructural changes of BGC823 cells. Next, we examined the role of BC001 on autophagy in BGC823 cells. Firstly, we evaluated the expression of Beclin1 and LC3II, which are indicators of autophagosome formation (12). As shown in Fig. 3A, no notable changes were reported in the expression of Beclin1 and LC3II in BC001 (0.1, 1.0, 10, 100 µg/ml)-treated BGC823 cells. In addition, the expression of autophagy-related protein P62 (a hallmark protein of autophagy) was also similar to that of the control group (Fig. 3B). These data indicated that BC001 has no effect on the autophagy in BGC823 cells. In contrast, in BGC823 cells treated with HCQ at 5 µg/ml, the conversion of LC3-I to LC3-II was promoted. In addition, the combination treatment of BC001 and HCQ had similar effects as HCQ treatment alone (Fig. 3C-E). To further analyze

how HCQ or BC001 affected the stepwise progression of autophagy, we constructed an mCherry-EGFP-LC3 reporter to observe the progression of autophagy flux. As shown in Fig. 4A, few yellow regions were observed in the untreated BGC823 cells. However, after 12 h of HCQ treatment, red and yellow regions were observed in the cells as compared with the control. Collectively, these results demonstrated that HCQ inhibited autophagy in BGC823 cells. Additionally, ultrastructural changes of BGC823 cells treated with HCQ and/or BC001 were investigated to identify morphological alterations of cell organelles and compartments. The results revealed swelling of the mitochondrial outer chambers in BGC823 cells treated with 5 µg/ml HCQ after 24 h. We also observed large fields of vacuoles and the dilatation of rough endoplasmic reticulum (rER) with formation of reticular rER clusters in cells. Furthermore, membrane-bound vesicles containing cytosolic materials or organelles were observed; degradative autophagic vacuoles were more abundant after HCQ treatment. However, BC001 had no notable effects on ultrastructural changes in BGC823 cells, while compared with HCQ group, combined treatment revealed no marked alterations (Fig. 4B). Collectively, BC001 (20 µg/ml) neither induced nor inhibited the autophagy in BGC823 cells, yet
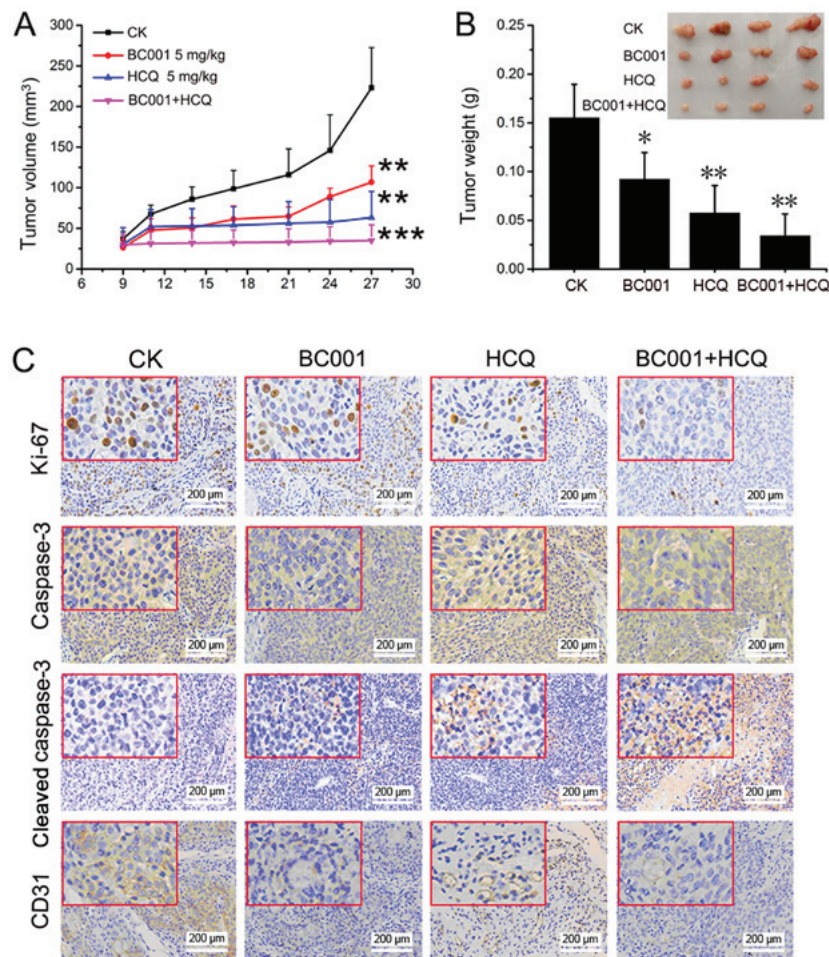
Figure 2. HCQ enhances the anticancer activity of BC001 *in vivo*. The tumor (A) volume and (B) weight of the different groups. (C) Relative Ki67, caspase-3, cle-caspase-3, CD31 expression was determined by immunohistochemical staining. Scale bar: 200 μm; magnification of insert, x3. *P<0.05, **P<0.01, ***P<0.001 vs. CK. Cle, cleaved; CK, control group.
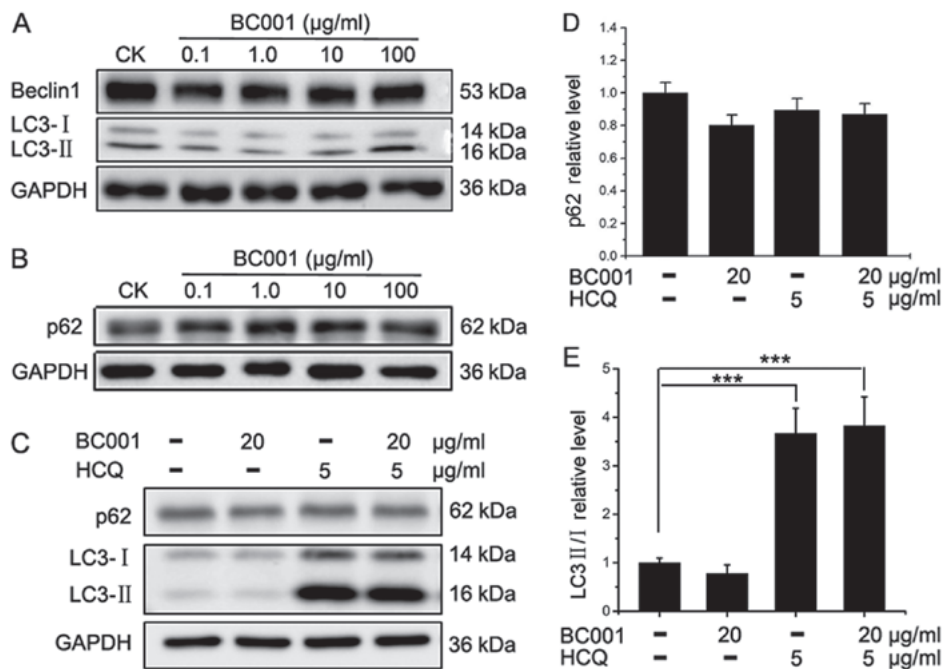

Figure 3. Effects of BC001 and/or HCQ on the expression of Beclin1, LC3 and p62. (A) The expression of Beclin1 and LC3 in BGC823 cells treated with BC001; (B) the expression of p62 in BGC823 cells treated with BC001. (C) The expression of p62 and LC3 in BGC823 cells treated with HCQ and/or BC001. (D) Relative expression levels of p62 in BGC823 cells treated with HCQ and/or BC001; (E) relative expression of LC3 II/I in BGC823 cells treated with HCQ and/or BC001. ***P<0.001 vs. CK. CK, control group; HCQ, hydroxychloroquine; LC3, microtubule-associated light chain 3.
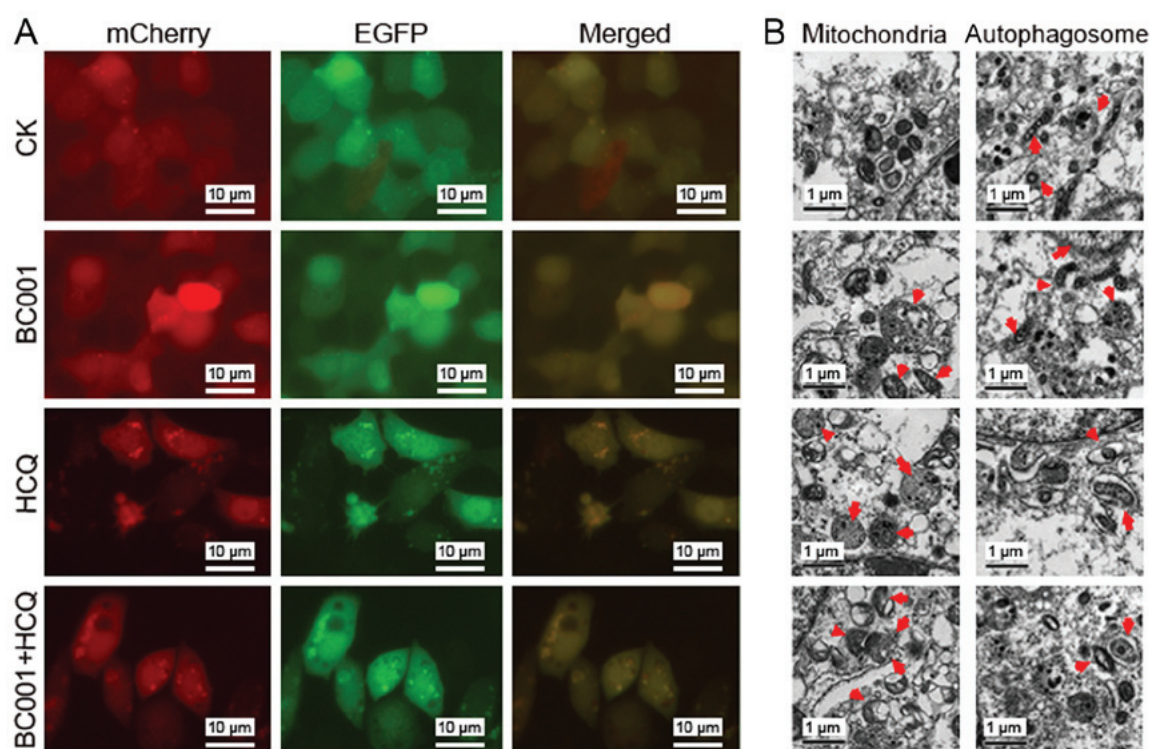
Figure 4. Effects of BC001 and/or HCQ on autophagy. (A) An mCherry-EGFP-LC3 reporter was constructed to observe the stepwise progression of autophagy in BGC823 cells. Scale bar: 10 μm. (B) Alterations in mitochondria and autophagosomes present in the cytoplasm were observed by transmission electron microscopy. The red arrows represent mitochondria or autophagosomes. Scale bar: 1 μm. CK, control group; EGFP, enhanced green fluorescent protein; HCQ, hydroxychloroquine.

HCQ could notably induce ultrastructural changes, which may contribute to the impairment of cellular lysosomal functions.

HCQ actives multiple pathways to promote the anticancer effects of BC001 in BGC823 cells. To understand how HCQ or BC001 inhibits proliferation and promotes cell death in BGC823 cells, we treated BGC823 cells with 5 μg/ml HCQ or 20 μg/ml BC001 for 48 h and performed global profiling of the transcriptome of HCQ or BC001-treated cells via RNA-Seq to identify the candidate genes. Following RNA-Seq analysis, a heatmap was generated to display the hierarchical clustering of genes in HCQ- and/ or BC001-treated cells (Fig. 5A). Our results revealed 679 significantly upregulated and 601 downregulated DEGs in HCQ-treated cells compared with control cells. In addition, 319 upregulated and 479 downregulated DEGs were reported for HCQ + BC001-treated cells compared with BC001-treated cells (Fig. 5B). Notably, a previous study have indicated an important role for lysosomes or the lysosome-dependent pathway after HCQ treatment (8). In the present study, we found that HCQ influenced certain autophagy and lysosomal genes, such as TP53INP1, IL1B, TNF, MEFV, USP36, IL6, NEU1, ABCA1, PCSK9, MBP, NEU3 (Fig. 5C and D). To further investigate the DEG-related pathways to reveal the potential mechanisms of HCQ, we performed enrichment analyses to identify possible associated pathways. The results showed that HCQ affected BGC823 cells via multiple pathways, including 'signal transduction', 'cancers' and 'immune system' (Fig. 6A). In addition, the combination of HCQ with BC001 was determined to mediate DEGs associated with

Table I. Sixteen differentially expressed genes in HCQ and/or BC001-treated BGC823 cells.

Gene	Log2[a]	Log2[b]	Log2[c]	Log2[d]	Log2[e]
RBM14-RBM4	-1.626	-2.868	-1.134	1.242	-1.734
CITED2	1.683	-1.050	1.597	2.733	-2.647
NEU3	-2.047	-3.233	-2.138	1.185	-1.095
SPINK5	-1.144	1.720	-1.328	-2.864	3.048
SPRED2	1.401	-1.111	1.370	2.513	-2.482
FOS	1.921	-1.428	2.193	3.349	-3.621
ADGRD1	1.814	-1.122	1.543	2.936	-2.665
SCHIP1	2.065	4.232	1.699	-2.167	2.533
IRS1	1.218	-1.362	1.441	2.580	-2.802
DLL4	3.233	-1.080	3.140	4.312	-4.219
CYP26B1	1.737	-1.158	1.379	2.895	-2.536
SHROOM3	1.296	-1.236	1.235	2.533	-2.471
SPRY4	3.244	-1.039	3.244	4.284	-4.284
TMEM164	-1.093	-2.196	-1.127	1.103	-1.069
ZBED3	-1.788	-3.010	-1.804	1.221	-1.206
EIF4EBP3	1.567	5.033	1.178	-3.466	3.855

[a]Log2 combination vs. CK; [b]log2 combination vs. HCQ; [c]log2 combination vs. BC001; [d]Log2 HCQ vs. CK; [e]log2 BC001 vs. HCQ. combination, BC001 + HCQ; HCQ, hydroxychloroquine.

'negative regulation of endothelial cell proliferation', 'blood vessel remodeling', 'cell surface receptor signaling pathway',
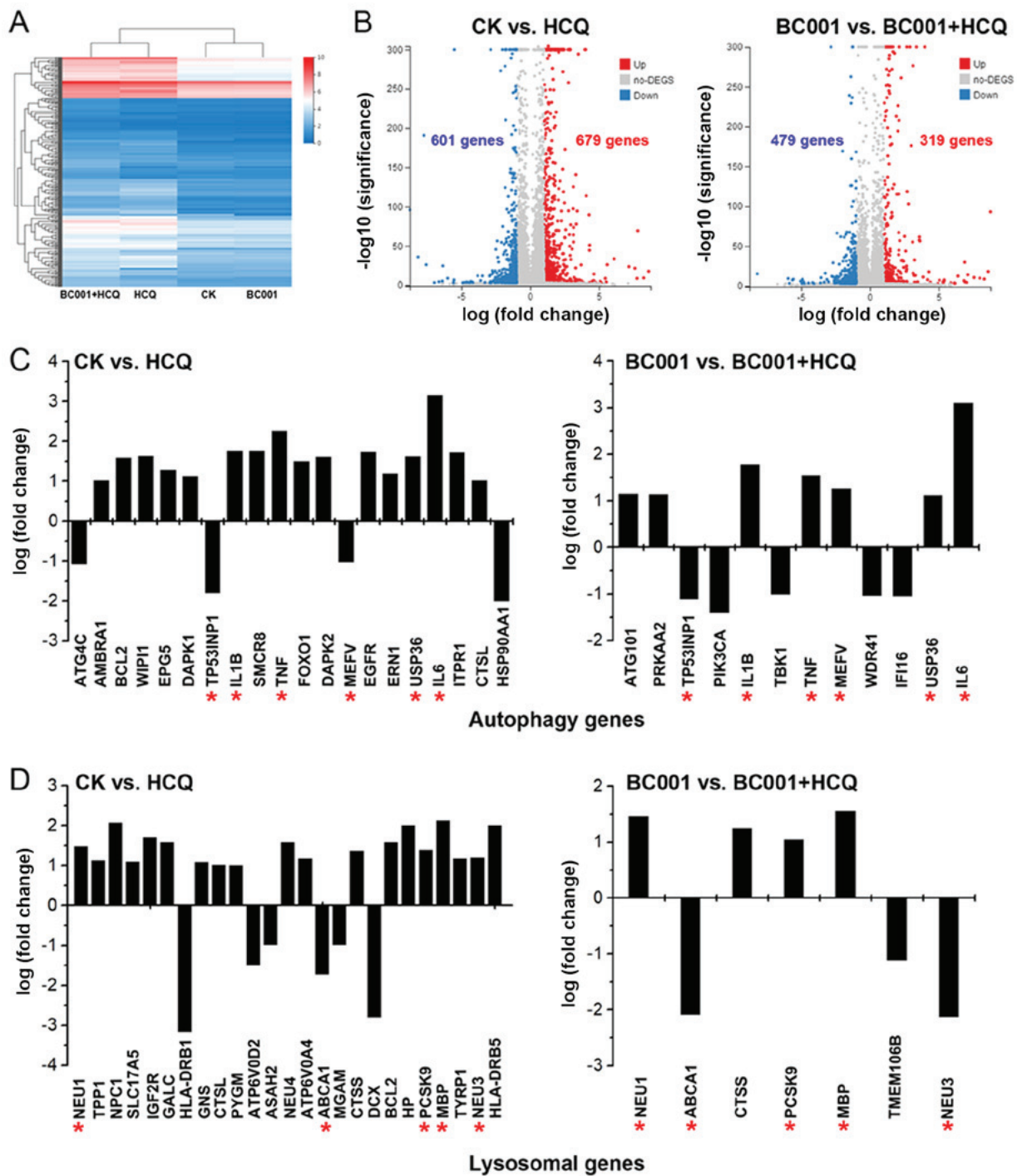
Figure 5. Transcriptome of HCQ and/or BC001-treated cells was analyzed via RNA-sequencing to identify DEGs. (A) Heatmap of the hierarchical clustering of genes in HCQ and/or BC001-treated cells; (B) 679 upregulated and 601 downregulated DEGs in HCQ-treated cells compared with control cells. (C) A total of 319 upregulated and 479 downregulated DEGs were reported in in HCQ + BC001-treated cells compared with BC001-treated cells; (D) HCQ affected the expression of some autophagy and lysosomal genes. * means these genes are the common DEGs. CK, control group; DEGs, differentially expressed genes; HCQ, hydroxychloroquine.

and 'notch receptor processing' associated with 'signal transduction', 'cancers' and 'immune system' (Fig. 6B). When analyzing the DEGs in different groups via a Venn diagram, 16 genes were identified (Table I and Fig. 6C). Compared with the BC001 group, we found 470 upregulated DEGs and 367 downregulated DEGs in the combined group, and highly interconnected 'hub' genes, including CXCL8, TNF, IL6, ICAM1 and FOS, were revealed by gene co-expression network analysis (Fig. 6D). These finding indicates HCQ

promotes the anticancer effect of BC001 in BGC823 cells partially via regulating immune responses.

Discussion

VEGFs and its receptors are important regulators of tumor angiogenesis (20), VEGFR2-targeting monoclonal antibody BC001 significantly inhibits angiogenesis and tumor growth (6); however, increasing evidence suggests that
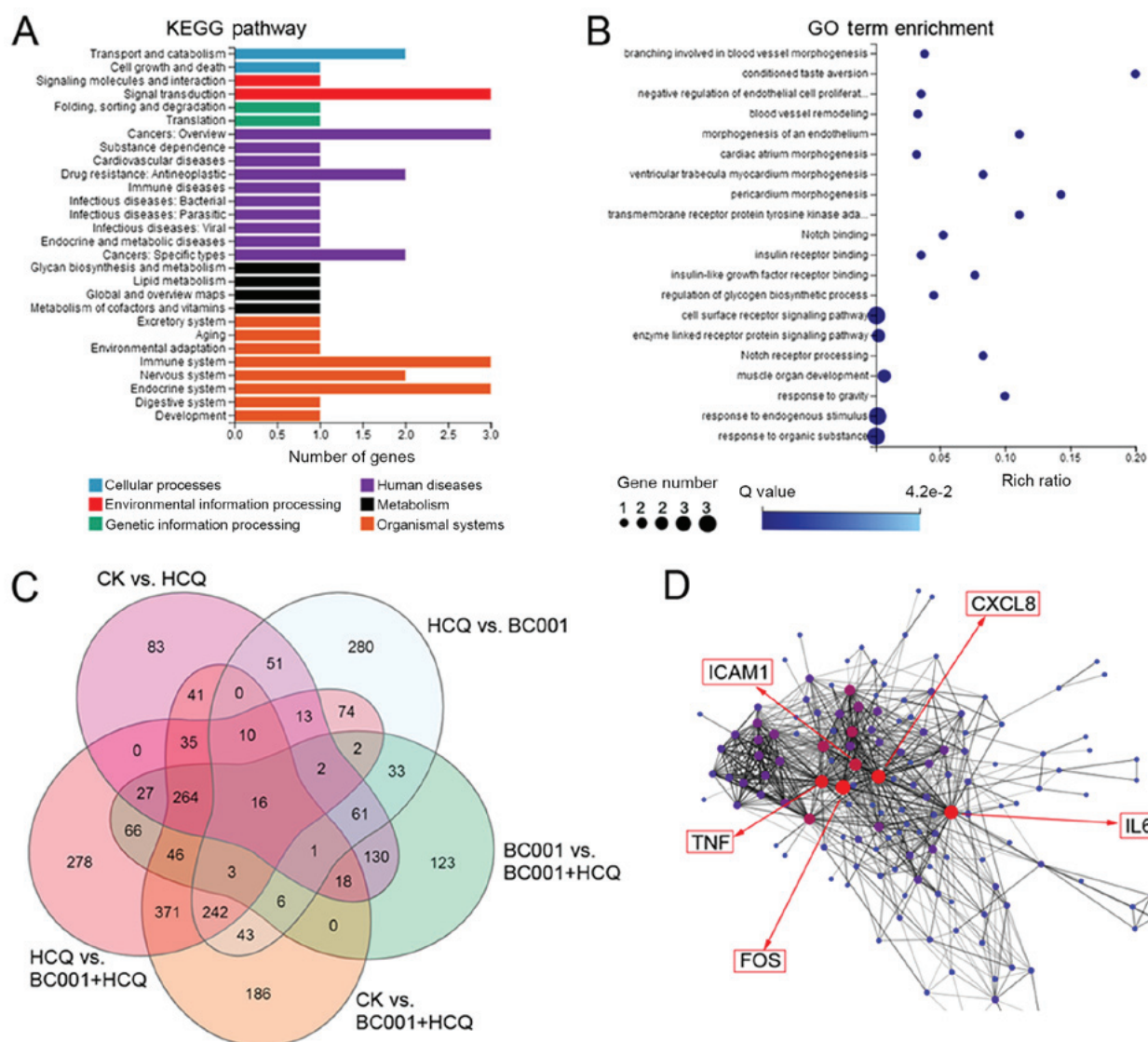
Figure 6. Investigation of the mechanism underlying the promoting effects of HCQ on the anticancer properties of BC001 in gastric cancer. (A) KEGG pathway enrichment analyses; (B) GO term enrichment. (C) Venn diagrams were established and 16 genes were identified; (D) gene co-expression networks revealed highly interconnected 'hub' genes in HCQ and/or BC001-treated cells. CK, control group; GO, Gene Ontology; HCQ, hydroxychloroquine; KEGG, Kyoto Encyclopedia of Genes and Genomes.

anti-angiogenic drugs could induce autophagy within tumors to mediate resistance (21), and HCQ can enhance the potential of some anticancer therapies (22).

In this study, our results suggested that HCQ inhibited the growth of BGC823 cells, and promoted the antiproliferative properties of BC001. In addition, HCQ promoted the apoptosis of BGC823 cells; the apoptotic rate was significantly increased in cells treated with both BC001 and HCQ. Additionally, the combination treatment exhibited higher inhibition potential than BC001 or HCQ against the growth of gastric cancer *in vivo*. Therefore, HCQ may enhance the anticancer activity of BC001 in gastric cancer. In addition, we found that BC001 neither induced nor inhibited the autophagy of BGC823 cells, whereas HCQ promoted the conversion of LC3-I to LC3-II, induced swelling of mitochondrial outer chambers, and promoted the formation of reticular rER clusters and degradative autophagic vacuoles. Our findings suggest that HCQ impaired the basal autophagic flux and inhibited autophagy, but BC001 did not affect HCQ-inhibited autophagy.

To understand how HCQ or BC001 inhibits the growth of gastric cancer, we used RNA-Seq to identify DEGs in BGC823 cells treated with HCQ and/or BC001. HCQ was determined to have influenced the expression of certain autophagy genes (TP53INP1, IL1B, TNF, MEFV, USP36, IL6) and lysosomal genes (NEU1, ABCA1, PCSK9, MBP, NEU3). Additionally, the results of enrichment analyses indicated that HCQ not only inhibited gastric cancer via regulating autophagy and lysosomal genes, but also via multiple pathways, including 'negative regula-tion of endothelial cell proliferation', 'blood vessel remodeling', 'cell surface receptor signaling pathway' and 'notch receptor processing' associated with 'signal transduction', 'cancers' and 'immune system'. Furthermore, 16 genes (RBM14-RBM4, Cbp/p300-interacting transactivator 2, NEU3, serine pepti-dase inhibitor, Kazal type 5, sprout related EVH1 domain containing 2, FOS, adhesion G protein-coupled receptor D1, Schwannomin-interacting protein 1, insulin receptor substrate 1, δ-like protein 4 precursor, cytochrome P450 family 26 subfamily B member 1, shroom family member 3, sprouty RTK

signaling antagonist, transmembrane protein 164, zinc finger BED domain-containing protein 3, eukaryotic translation initiation factor 4E binding protein 3) were significant DEGs between groups treated by HCQ or HCQ + BC001. Consistent with recent reports, chloroquine modulates the antitumor immune response (23,24); in our study, co-expression networks showed that CXCL8, TNF, IL6, ICAM1 and FOS may be highly interconnected 'hub' genes. IL-6 and TNFα are pro-inflammatory cytokines. Emerging evidence has revealed that the expression of IL-6 and TNFα was significantly increased in gastric cancer, which promoted gastric cancer cell migration and invasion (25). In addition, HCQ disrupted the CXCR/CXCL axis which could induce invasion and metastasis of malignant melanoma in an autophagy-independent manner (26). ICAM1, which has been related to the aggressive nature of gastric cancer, can be induced by proinflammatory cytokines (27). FOS, a proto-oncogene, has been implicated as a regulator of cell proliferation, cell death, differentiation and transformation (28).

In conclusion, our results suggested that HCQ increased anticancer activity of BC001 in gastric cancer, suggesting that the combined treatment of HCQ and BC001 may be considered as a promising approach for the treatment of gastric cancer. However, further investigation is necessary to validate the combined mechanisms.

Availability of data and materials

All data are included in this published article.

Authors' contributions

WW and LL performed the experiments and wrote the paper, YZ, XT, QY, FG, and JJ conceived and designed the experiments and edited the manuscript, ZX, XT, ZY and XY analyzed the data, GZ and QF revised the manuscript. All authors read and approved the final manuscript.

Ethics approval and consent to participate

All animal experiments were performed following the approval of the Ethical Committee of Zhejiang Provincial People's Hospital (approval no. KY2015156), and according to the Guideline for the Care and Use of Laboratory Animals (29).

Patient consent for publication

Not applicable.

Competing interests

The authors declare no conflict of interest.

References

1. Bray F, Ferlay J, Soerjomataram I, Siegel RL, Torre LA and Jemal A: Global cancer statistics 2018: GLOBOCAN estimates of incidence and mortality worldwide for 36 cancers in 185 countries. CA Cancer J Clin 68: 394-424, 2018.
2. Sharma MR, Joshi SS, Karrison TG, Allen K, Suh G, Marsh R, Kozloff MF, Polite BN, Catenacci DVT and Kindler HLA: A UGT1A1 genotype-guided dosing study of modified FOLFIRINOX in previously untreated patients with advanced gastrointestinal malignancies. Cancer 125: 1629-1636, 2019.
3. Viallard C and Larrivée B: Tumor angiogenesis and vascular normalization: Alternative therapeutic targets. Angiogenesis 20: 409-426, 2017.
4. Gilbert MR, Dignam JJ, Armstrong TS, Wefel JS, Blumenthal DT, Vogelbaum MA, Colman H, Chakravarti A, Pugh S, Won M, et al: A randomized trial of bevacizumab for newly diagnosed glioblastoma. N Engl J Med 370: 699-708, 2014.
5. Javle M, Smyth EC and Chau I: Ramucirumab: Successfully targeting angiogenesis in gastric cancer. Clin Cancer Res 20: 5875-5881, 2014.
6. Xuan ZX, Li LN, Zhang Q, Xu CW, Yang DX, Yuan Y, An YH, Wang SS, Li XW and Yuan SJ: Fully human VEGFR2 monoclonal antibody BC001 attenuates tumor angiogenesis and inhibits tumor growth. Int J Oncol 45: 2411-2420, 2014.
7. Han K, Jin J, Maia M, Lowe J, Sersch MA and Allison DE: Lower exposure and faster clearance of bevacizumab in gastric cancer and the impact of patient variables: Analysis of individual data from AVAGAST phase III trial. AAPS J 16: 1056-1063, 2014.
8. Hu Y-L, Jahangiri A, De Lay M and Aghi MK: Hypoxia-induced tumor cell autophagy mediates resistance to anti-angiogenic therapy. Autophagy 8: 979-981, 2012.
9. Levy JMM, Towers CG andThorburn A: Targeting autophagy in cancer. Nat Rev Cancer 17: 528-542, 2017.
10. Mokarram P, Albokashy M, Zarghooni M, Moosavi MA, Sepehri Z, Chen QM, Hudecki A, Sargazi A, Alizadeh J, Moghadam AR, et al: New frontiers in the treatment of colorectal cancer: Autophagy and the unfolded protein response as promising targets. Autophagy 13: 781-819, 2017.
11. Cook KL, Warri A, Soto-Pantoja DR, Clarke PA, Cruz MI, Zwart A and Clarke R: Hydroxychloroquine inhibits autophagy to potentiate antiestrogen responsiveness in ER⁺ breast cancer. Clin Cancer Res 20: 3222-3232, 2014.
12. Rosenfeld MR, Ye X, Supko JG, Desideri S, Grossman SA, Brem S, Mikkelson T, Wang D, Chang YC, Hu J, et al: A phase I/II trial of hydroxychloroquine in conjunction with radiation therapy and concurrent and adjuvant temozolomide in patients with newly diagnosed glioblastoma multiforme. Autophagy 10: 1359-1368, 2014.
13. Selvakumaran M, Amaravadi RK, Vasilevskaya IA and O'Dwyer PJ: Autophagy inhibition sensitizes colon cancer cells to antiangiogenic and cytotoxic therapy. Clin Cancer Res 19: 2995-3007, 2013.
14. Chiu CH, Lei KF, Yeh WL, Chen P, Chan YS, Hsu KY and Chen AC: Comparison between xCELLigence biosensor technology and conventional cell culture system for real-time monitoring human tenocytes proliferation and drugs cytotoxicity screening. J Orthop Surg Res 12: 149, 2017.
15. Wang Y, Zhang J, Huang Z-H, Huang X-H, Zheng W-B, Yin X-F, Li Y-L, Li B and He Q-Y: Isodeoxyelephantopin induces protective autophagy in lung cancer cells via Nrf2-p62-keap1 feedback loop. Cell Death Dis 8: e2876, 2017.
16. Gump JM and Thorburn A: Sorting cells for basal and induced autophagic flux by quantitative ratiometric flow cytometry. Autophagy 10: 1327-1334, 2014.
17. Alirezaei M, Flynn CT, Wood MR, Harkins S and Whitton JL: Coxsackievirus can exploit LC3 in both autophagy-dependent and -independent manners in vivo. Autophagy 11: 1389-1407, 2015.

18. Dong J-K, Lei H-M, Liang Q, Tang Y-B, Zhou Y, Wang Y, Zhang S, Li W-B, Tong Y, Zhuang G, *et al*: Overcoming erlotinib resistance in EGFR mutation-positive lung adenocarcinomas through repression of phosphoglycerate dehydrogenase. Theranostics 8: 1808-1823, 2018.
19. Han J, Chen M, Wang Y, Gong B, Zhuang T, Liang L and Qiao H: Identification of biomarkers based on differentially expressed genes in papillary thyroid carcinoma. Sci Rep 8: 9912, 2018.
20. Pirola L, Ciesielski O and Balcerczyk A: The methylation status of the epigenome: Its emerging role in the regulation of tumor angiogenesis and tumor growth, and potential for drug targeting. Cancers (Basel) 10: 268, 2018.
21. Mulcahy Levy JM, Zahedi S, Griesinger AM, Morin A, Davies KD, Aisner DL, Kleinschmidt-DeMasters BK, Fitzwalter BE, Goodall ML, Thorburn J, *et al*: Autophagy inhibition overcomes multiple mechanisms of resistance to BRAF inhibition in brain tumors. eLife 6: e19671, 2017.
22. Zhao Z, Xia G, Li N, Su R, Chen X and Zhong L: Autophagy inhibition promotes bevacizumab-induced apoptosis and proliferation inhibition in colorectal cancer cells. J Cancer 9: 3407-3416, 2018.
23. Maes H, Kuchnio A, Carmeliet P and Agostinis P: Chloroquine anticancer activity is mediated by autophagy-independent effects on the tumor vasculature. Mol Cell Oncol 3: e970097, 2015.
24. Chen D, Xie J, Fiskesund R, Dong W, Liang X, Lv J, Jin X, Liu J, Mo S, Zhang T, *et al*: Chloroquine modulates antitumor immune response by resetting tumor-associated macrophages toward M1 phenotype. Nat Commun 9: 873, 2018.
25. Huang H, Wang Y, Cao Y, Wu B, Li Y, Fan L, Tan Z, Jiang Y, Tang J, Hu J, *et al*: Interleukin-6, tumor necrosis factor-alpha and receptor activator of nuclear factor kappa ligand are elevated in hypertrophic gastric mucosa of pachydermoperiostosis. Sci Rep 7: 9686, 2017.
26. Yin S, Xia C, Wang Y, Wan D, Rao J, Tang X, Wei J, Wang X, Li M, Zhang Z, *et al*: Dual receptor recognizing liposomes containing paclitaxel and hydroxychloroquine for primary and metastatic melanoma treatment via autophagy-dependent and independent pathways. J Control Release 288: 148-160, 2018.
27. Figenschau SL, Knutsen E, Urbarova I, Fenton C, Elston B, Perander M, Mortensen ES and Fenton KA: ICAM1 expression is induced by proinflammatory cytokines and associated with TLS formation in aggressive breast cancer subtypes. Sci Rep 8: 11720, 2018.
28. van IJzendoorn DGP, Forghany Z, Liebelt F, Vertegaal AC, Jochemsen AG, Bovée JVMG, Szuhai K and Baker DA: Functional analyses of a human vascular tumor FOS variant identify a novel degradation mechanism and a link to tumorigenesis. J Biol Chem 292: 21282-21290, 2017.
29. National Research Council: Guide for the Care and Use of Laboratory Animals. 8th edition. The National Academies Press, Washington, DC, 2011.